Numerical Study of Low Frequency G-jitter Effect on Thermal Diffusion

Y. Yan[1], V. Shevtsova[2], M. Z. Saghir[1]

Abstract: Convection has a major impact on diffusion in fluid mixtures either on the Earth or in the microgravity condition. G-jitters, as the primary source that induces the vibrational convection in space laboratories, should be studied thoroughly in order to improve the diffusion-dominated fluid science experiments. In this paper we consider the effect of g-jitters on thermal diffusion. The mixture water-isopropanol (90:10 wt%) bounded in a cubic cell is simulated with a lateral heating and various vibration conditions. The fluid flow, concentration and temperature distributions are thoroughly analyzed for different g-jitter scenarios. It is shown that the overall effect of vibrations on diffusion can be regarded basically as a nonlinear interaction between the effects caused by each individual g-jitter component. In the presence of large static residual gravity, the effect of convection on diffusion is very significant, thus resulting in a limited Soret separation. On the contrary, the importance of periodic vibration on diffusion changes according to the frequency. Low frequency vibrations exhibit a more dangerous effect on diffusion measurements with respect to high frequency vibrations. The dependence of the Soret separation on frequency and the driving mechanisms at low frequency g-jitters are discussed on the basis of these behaviors.

keyword: Thermal diffusion, Convection, Numerical simulation, Finite volume, Microgravity, G-jitter

1 Introduction

The phenomenon related to a convection-free mixture that separates under a temperature gradient is known as "thermal diffusion", or "Soret effect" for binary mixtures. This phenomenon may occur in both liquid and gaseous mixtures. For years liquid thermal diffusion has been studied extensively with an intention to understand a variety of engineering and scientific problems that it associates, such as the compositional variation in hydrocarbon reservoirs, hydrodynamic instability of mixtures, mineral migrations and mass transport in living matters.

The thermal diffusion process characterizes the coupling of diffusion fluxes driven by the temperature and concentration gradients. It is commonly evaluated by the thermal diffusion coefficient, or Soret coefficient for binary mixtures. In reality, a buoyancy force usually exists simultaneously and drives the natural convection. This phenomenon is referred to as double diffusion convection. On the Earth, the buoyancy convection is so strong that it makes the ground-based experiments extremely difficult. Therefore, performing experiments in a convection-free environment seems to be a good opportunity to bypass this problem. Space laboratories offers microgravity environment, which makes it possible to achieve somewhat true diffusion conditions. However, due to the existence of static and oscillatory residual accelerations (g-jitters) in space laboratories, diffusion experiments are affected by the g-jitter induced convection. Although much weaker compared to that on the Earth, this convection has to be fully considered to ensure the accuracy of experiments. G-jitters have a wide spectrum of amplitudes and frequencies. Their effect on diffusion varies depending on both amplitude and frequency. Theoretical study of the g-jitter effect at different conditions therefore becomes essential in supporting space experiments and better understanding the measurement results.

Recent studies concerning the effect of different gravity modulations on convection have been reported by several researchers. For example, Farooq and Homsy (1994) investigated streaming in a square cavity where a lateral temperature gradient interacts with a constant gravity field modulated by small harmonic oscillations. They found that under certain parametric conditions with finite frequency and moderate Pr number, the periodic motion interacts with the instabilities associated with the base flow and causes resonances, which increases in strength as Ra increases. At low frequencies the

[1] Ryerson University, Dept. Mechanical Engineering, 350 Victoria St., Toronto, M5B 2K3, ON, Canada
[2] MRC, CP-165/62, Universit'e Libre de Bruxelles, 50, Av. F.D.Roosevelt, B-1050, Brussels, Belgium

streaming flow shows marked structural changes as Ra increases. Farooq and Homsy (1996) studied the dynamics of a differentially-heated, gravity-modulated slot and observed parametric resonance, which leads to instability of the flow. The stability boundary were found to depend on the frequency and the amplitude of the modulation. Chen and Chen (1999) examined the effect of gravity modulation on the stability characteristics of convection in a differentially heat infinite slot for fluids with $Pr = 1$ and $Pr = 25$. For both kinds of fluids, they observed that the instability mode switching is a dynamic response to the periodic forcing and is independent of the dominant mechanism for instability. Rees and Pop (2001) investigated the influence of periodical gravity modulation on free convection in porous media. By examining the detailed effect of the g-jitter' amplitude and frequency on the flow and heat transfer characteristics, they have stated that the low-frequency g-jitter has a significant effect on the stability of the system. For large values of the forcing frequency, the numerical evidence suggests that the flow is unaffected by g-jitter at leading order, while at small values of the frequency, the heat transfer response is almost exactly in phase with the gravitational acceleration.

Some researchers, in particular, have focused on the effect of low frequency vibrations on convection. Hirata et al (2001) have recently analyzed the system response of buoyancy driven fluid to oscillatory accelerations in a microgravity environment by means of a fully nonlinear numerical simulation for a two-dimensional, bottom-heated, square cavity. They have found that, in the range tested, time evolutions exhibit synchronous, 1/2-subharmonic and non-periodic responses, and the flow pattern is characterized mainly by a one- or two- cellular structure according to the vibrational Rayleigh number Ra and the dimensionless angular frequency ω. As ω increases or Ra decreases, convection becomes more stable. The non-periodic responses appear for $Ra > 5 \times 10^4$ in the flow regimes as the result of transitions between flow patterns.

In earlier studies, transition to chaos at $Ra = 10^4$ for a laterally heated square cavity was reported by Lizée and Alexander (1997), who considered the onset of chaotic thermovibrational convection in a laterally heated square cavity. They stated that the intermittent transitional flows exhibit strong nonlinearities and cannot be considered in terms of a small perturbation superimposed on a mean flow that is close to the $Ra_v = 0$ flow.

More recently, Savino and Lappa (2003) have tried to build new sets of reduced equations valid at relatively low frequencies by direct numerical simulation of the Navier-Stokes equations with an oscillatory body force in the momentum equation. In practice, these different sets of equations, given by the omission of some terms, have been obtained through an "a posteriori" analysis of the different diffusive, convective and production terms in the Navier-Stocks equations.

Other recent articles that have discussed vibrations in general and depicted in detail the structure of steady three-dimensional gravitational flows may be found in Lappa (2005a), Lappa (2005b), and Melnikov and Shevtsova (2005).

Lappa (2005a) has presented a comprehensive review and critical analysis on the possible strategies for the control and stabilization of Marangoni flow in laterally heated floating zones; in particular, the application of forced high-frequency vibrations has been considered as a possible and economic means to induce flow stabilization.

Lappa (2005b) has investigated the different scenarios that arise in cubical and shallow cavities filled with silicon melt in terms of the structure of the convective field and possible stable and unstable regimes within the framework of numerical solution of the non-linear balance equations through multiprocessor computations. Various types of convective mechanisms under different heating conditions have been thoroughly discussed to illustrate the possible three-dimensional patterns of symmetry.

Melnikov and Shevtsova (2005) have numerically studied the buoyancy-driven convective flows in a laterally heated cubic enclosure through a liquid particles tracing technique. In particular they have shown that two-dimensional approach can not provide a clear picture of the three-dimension convection, especially at large Pr number.

Several articles also exist where attention was focused on double-diffusion convection, for example, Monti and Savino (1995), Shu et al (2001), Chacha et al. (2002), and Chacha and Saghir (2005). Monti and Savino (1995) studied a general case of quasi steady residual gravities superimposed to high frequency-small amplitude g-jitters by means of a time-averaged formulation in order to evaluate the maximum allowable high fre-

quency g-jitters that specific microgravity experiments can tolerate. They numerically analyzed the thermo-fluid-dynamic distortions as a function of the classical Rayleigh number for steady gravities, and of the vibrational Rayleigh number, for high frequency g-jitters. On the basis of their results, the g-tolerability domain was drawn for a study on thermal diffusion in a fluid cell.

Shu et al (2001) utilized the finite element method to study the double-diffusion convection driven by g-jitter in a microgravity environment for binary alloy melt systems. Their computations include various vibration conditions, i.e., idealized single-frequency and multifrequency g-jitter as well as the real g-jitter data taken during an actual Space Shuttle flight. They have found that the disturbance of the concentration field is pronounced, and with an increase in g-jitter force (or amplitude), the nonlinear convective effects become much more obvious, which in turn drastically change the concentration fields.

Chacha et al. (2002) investigated the thermal diffusion in a binary mixture of methane and n-butane subject to g-jitters with moderately high frequency. For various configurations, they noticed that the g-jitter causes mixing and overcomes the Soret effect in the cavity. The flow was found to respond synchronously to the oscillatory accelerations. More recently, Chacha and Saghir (2005) have studied the effect of the time dependent vertical gravity vector on the mass diffusion in a binary fluid mixture in a rigid rectangular cell subject to a lateral temperature gradient. Their numerical results show that the g-jitter reduces the compositional variation; and it is essential to eliminate both residual gravities and g-jitter levels to achieve nearly ideal diffusive conditions when their directions are orthogonal to that of the temperature gradient. They have also found that the Soret number oscillates with time at the same frequency as the original excitation. However, the backflow disturbs this variation and makes it non-sinusoidal in shape. Shevtsova et.al. (submitted) have studied the influence of different vibration conditions on thermal diffusion for a binary mixture. They have noticed that the effect of the combined static and oscillatory vibrations on diffusion is not a simple summation of fields generated by each individual vibration component. The vibrational mean fields, as well as the "convective" mean fields with and without the static gravity are different.

The studies cited in the foregoing text are valuable examples of efforts provided to discern the characteristics of double diffusion convection and thus to improve our understanding of the g-jitter effect on diffusion process. However, more precise knowledge is still needed to uncover the underlying mechanisms and to determine the range of the most harmful frequencies in space experiments. This requires extensive numerical work to be done for g-jitters in a variety of frequencies. So far, most of studies have been focused on (moderate) high frequency vibrations. Very limited information is available for the double-diffusion convection under low frequency vibrations. Furthermore, it is not clear that under multiple-frequency g-jitter conditions, whether the effect of vibration is amplitude dependent, frequency dependent or both play important roles through somewhat interaction still remains a question mark. It is expected that further numerical work will help to discover the physical difference of the impacts of vibration frequencies on diffusion. It will also contribute to a larger database, through which the diffusion theories may be validated more generally and thoroughly.

The main purpose of this research is to evaluate the g-jitter effect on thermal diffusion with a focus on low frequency g-jitters. Single-frequency g-jitters represent the idealized situation. Although they rarely happen in real microgravity environment, they are very essential to gain fundamental insights into the mechanisms of double-diffusive convection. In this paper we numerically study the thermal diffusion process of a binary mixture water-isopropanol (90:10 wt%) in a cubical cell in the presence of g-jitters ranging from 0.001Hz to 0.025Hz. These frequencies in general fall into the low-frequency spectrum of the microaccelerations onboard the Foton satellites [Sazonov et al (2004)]. A lateral heating condition is applied to the fluid system. The finite volume method is used to solve the Boussinesq approximated governing equations. The effect of g-jitter frequency and amplitude on the intensity of the fluid flow, heat and mass transfer, and Soret separation are investigated in a quite exhaustive way.

2 Mathematical model

An initially homogenous binary mixture, water-isopropanol (90:10 wt%) is filled in a $10 \times 10 \times 10 (\text{mm}^3)$ cubical cavity. Fig. 1 illustrates the physical problem. The two opposite side walls are kept in constant temperatures, $T_{hot} = 303.15K$ and $T_{cold} = 293.15K$, respectively. All other walls are thermally insulated. The cubical

Table 1 : Physical properties of the mixture at $T_0 = 298.15K$ and $p_0 = 1.013 \times 10^5 Pa$

Density ρ_0	984 kg/m^3
Kinematic viscosity ν	1.41×10^{-6}m^2/s
Specific heat c_P	3990.5 J/(kg K)
Thermal conductivity k	0.522 W/(m K)
Thermal expansion coefficient β_T	3.1×10^{-4} 1/K
Volumetric concentration expansion coefficient β_c	0.1386
Molecular diffusion coefficient D_c	$8.7 \times 10^{-10} m^2/s$
Soret coefficient S_{T_con} (conventional definition)	-10.6×10^{-3}1/K (21°C)
	-7.63×10^{-3}1/K (37.5°C)
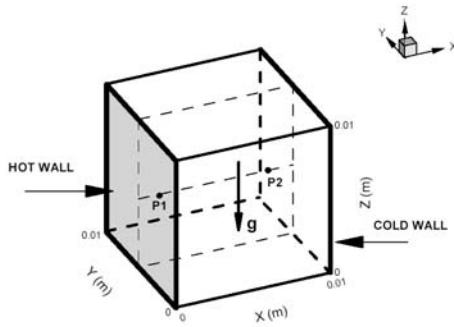
Figure 1 : Physical model

cavity is rigid and impermeable to matter. The system is subject to static and/or oscillatory gravities, which are oriented perpendicular to the temperature gradient, i.e., in the Z (vertical) direction. Physical properties of the mixture are summarized in Tab. 1.

2.1 Governing equations

The problem of double diffusion convection is governed by the mass conservation, species conservation, energy and momentum equations. Both molecular and thermal diffusion coefficients are assumed to be constant in the simulation. The Boussinesq approximation is applied, therefore the equation of state may be simplified as:

$$\rho = \rho_0 \left[1 - \beta_T \left(T - T_0 \right) + \beta_c \left(c - c_0 \right) \right] \qquad (1)$$

The governing equations take the form:

$$\nabla \cdot \vec{u} = 0 \qquad (2)$$

$$\frac{Dc}{Dt} = D_c \nabla^2 c + D_T \nabla^2 T \qquad (3)$$

$$\frac{DT}{Dt} = \frac{k}{\rho c_p} \nabla^2 T \qquad (4)$$

$$\frac{D\vec{u}}{Dt} = -\frac{1}{\rho} \nabla p + \nu \nabla^2 \vec{u} + \vec{g} \qquad (5)$$

where the operator $\frac{D}{Dt} = \frac{\partial}{\partial t} + u\frac{\partial}{\partial x} + v\frac{\partial}{\partial y} + w\frac{\partial}{\partial z}$; ρ is the density; T is the temperature; c is the mass concentration of water (carrier); p is the pressure; $\vec{u}$ is the velocity vector; $\vec{u} = u \cdot \vec{i} + v \cdot \vec{j} + w \cdot \vec{k}$; c_P is the specific heat; k is the thermal conductivity; ν is the kinematic viscosity; β_T is the thermal expansion coefficient; β_c is the volumetric concentration expansion coefficient; D_c is the molecular diffusion coefficient; D_T is the thermal diffusion coefficient; $\vec{g}$ is the gravity vector, see Eq. 17; and the subscript 0 denotes properties at the initial state.

It should be mentioned that D_T in Eq. 3 adopts the definition in the Firoozabadi model [Shukla and Firoozabadi (1998)]. It relates to the conventional definition, D_{T_con}, as follows:

$$D_T = c_0(1 - c_0)D_{T\_con} \qquad (6)$$

therefore the Soret coefficient, S_T, in this study relates to the conventional definition, S_{T_con}, as follows:

$$S_T = c_0(1 - c_0)S_{T\_con} \qquad (7)$$

2.2 Boundary and initial conditions

The no flow and no slip boundary conditions are applied to the side walls; and there are no reactions inside the cavity and no mass flux through the side walls. The vertical walls have constant temperatures, and other walls are assumed to be adiabatic. The boundary conditions are given by:

at $x = 0$, $x = L$:

$$u = 0 \tag{8}$$

$$J_x = D_c \frac{\partial c}{\partial x} + D_T \frac{\partial T}{\partial x} = 0 \tag{9}$$

$$T|_{x=0} = T_{hot} \quad , \quad T|_{x=L} = T_{cold} \tag{10}$$

at $y = 0$, $y = W$:

$$v = 0 \tag{11}$$

$$J_y = D_c \frac{\partial c}{\partial y} + D_T \frac{\partial T}{\partial y} = 0 \tag{12}$$

$$\frac{\partial T}{\partial y} = 0 \tag{13}$$

and at $z = 0$, $z = H$:

$$w = 0 \tag{14}$$

$$J_z = D_c \frac{\partial c}{\partial z} + D_T \frac{\partial T}{\partial z} = 0 \tag{15}$$

$$\frac{\partial T}{\partial z} = 0 \tag{16}$$

where J_x, J_y and J_z are the diffusion fluxes in the X, Y and Z directions, respectively; L, W, and H denote the length, width, and height of the cavity. The initial conditions are $\vec{u} = 0$, $c_0 = 0.9$, $p_0 = 1.013 \times 10^5 Pa$ and $T_0 = 298.15 K$ $(0 < x < L)$.

3 Numerical method

The set of governing equations, Eq. 1 to Eq. 5, contain seven unknowns, i.e, (u, v, w, ρ, p, T, c) to be solved for each mesh point in the cavity. In our model the finite volume method is used for discretizing the mass, momentum and energy equations along with the appropriate boundary and initial conditions. For solving the governing equations, the SIMPLE algorithm [Patankar (1980); Peyret and Taylor (1983)] is implemented. In this algorithm, the iteration process starts by using guessed initial pressure and velocity fields. Then, solving the continuity equation, a pressure correction field is obtained, which, in turn, is used to update the velocity and pressure field. This procedure is iterated until the convergence is achieved. More details of the numerical procedure may be found in Chacha et al (2003). The mesh sensitivity analysis has been conducted with the Nusselt number at the hot and cold walls as the evaluation criterion, see Chacha et al (2003). The optimal mesh $19 \times 9 \times 19$ was used to obtain all the results presented in the following sections.

4 Results and discussion

In this paper we have studied five different g-jitter cases with respect to the amplitude and frequency as well as static residual gravity cases ranging from 0 to 10^{-2} g_0. Tab. 2 lists the details of these g-jitter cases. The gravity vector takes the form:

$$\vec{g} = -[g_{st} + g_{vib}\sin(2\pi f t)] \cdot \vec{k} \tag{17}$$

where g_{st} is the static component of the g-jitter; g_{vib} is the amplitude of the oscillatory component of the g-jitter; f is the g-jitter frequency; and the sign minus denotes that the gravity is in the opposite direction of Z axis.

Table 2 : G-jitter cases simulated in this study

	Frequency	g_{st}	g_{vib}
Case 1	0.025 Hz		
Case 2	0.005 Hz	0	
Case 3	0.001 Hz		10^{-3} g_0
Case 4	0.025 Hz	10^{-4} g_0	
Case 5	0.001 Hz		

In the following sections we will discuss how the static residual gravity, pure oscillatory g-jitter, and the combination of both affect the diffusion process. We will also analyze the effect of g-jitter frequency on diffusion. The separation rate, Sr, has been used to quantify the components separation. It is defined with respect to the maximal possible separation at zero gravity, Δc , as follows:

$$Sr = (\tilde{c}_{cold} - \tilde{c}_{hot})/\Delta c \tag{18}$$

and

$$\Delta c = c_0(1 - c_0)S_{T\_con}\Delta T \tag{19}$$

where ΔT is the initial temperature difference between the hot and cold walls. $\tilde{c}_{cold}$ and $\tilde{c}_{hot}$ are average concentrations of water at the cold and hot walls, respectively, when the system reaches the quasi steady state. At ideal zero gravity, $Sr = 1$. In the presence of g-jitters, $Sr < 1$. The more the Soret separation departs from 1, the more strongly the convection affects the diffusion. The effect of convection on diffusion is also reflected in temperature profiles. The maximum deviation of the temperature profile from the linear distribution, δT , is thus examined, which is defined as follows:

$$\delta T = \max\left[abs(T_{full} - T_{linear})\right] \tag{20}$$

(a): 10^{-6} g_0

(b): 10^{-4} g_0

(c): 10^{-3} g_0
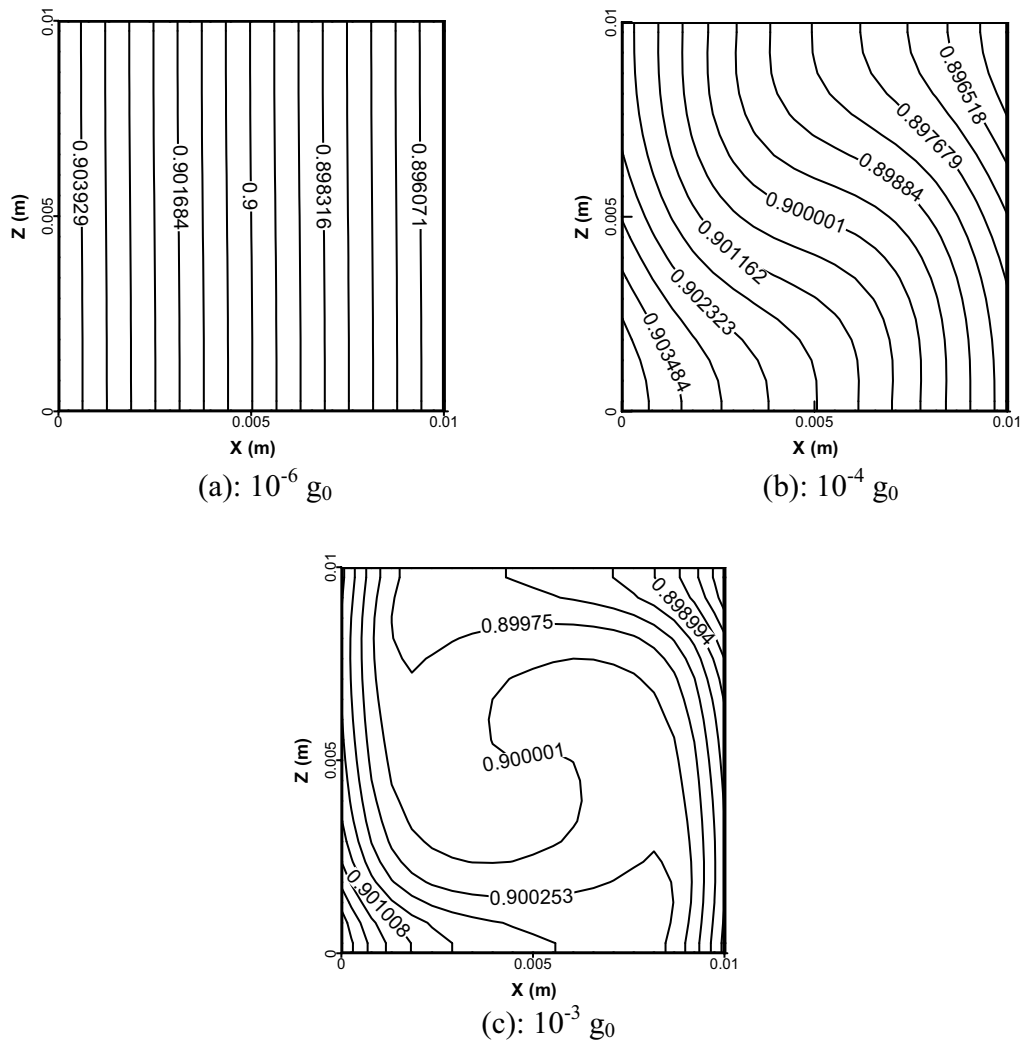
Figure 2 : Comparison of water concentration contours at different levels of gravity
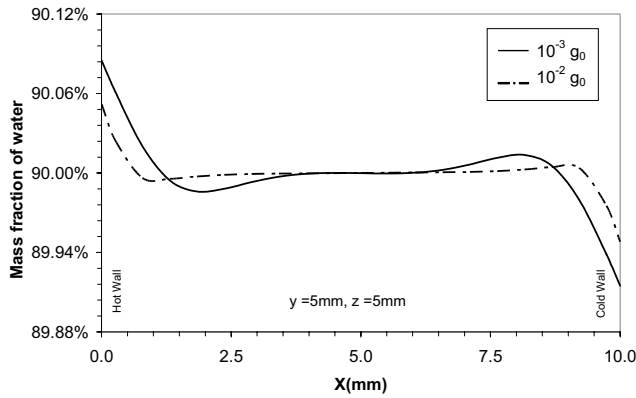
where T_{full} is the local temperature when the system reaches the quasi steady state; and T_{linear} is the temperature at the same location assuming that the zero gravity condition is applied.

Prior to discussion, it is necessary to address the characteristic times, namely, thermal characteristic time $\tau_{th} = L^2/a$, molecular diffusion characteristic time $\tau_D = L^2/D_c$, and viscous characteristic time $\tau_v = L^2/v$. τ_{th} measures how quickly materials respond to thermal changes and reach to a new equilibrium. It depends on the characteristic length of the cavity L and the thermal diffusivity of the material a ($a = k/\rho c_p$). For water-isopropanol in the cubic cell in this study, $\tau_{th} \approx 770s$. Simultaneous to the heat transfer, mass transfer occurs along the temperature gradient, however, much more

slowly than the thermal process. Its characteristic time is usually much higher than the thermal characteristic time. In this study $\tau_D \approx 115 \times 10^3 s$. Viscous characteristic time usually has a much smaller value than the thermal and molecular diffusion characteristic times. In this study $\tau_v \approx 70s$.

4.1 Effect of static residual gravities

When only the static residual gravity exists, the buoyancy force constantly acts on the mixture without changing direction. It has a negative effect on thermal diffusion; the degree of its effect depends on the magnitude of the residual gravity. Fig. 2 compares the contours of water distribution in the X-Z middle cross-section of the cubic cell at different levels of residual gravity. With

Figure 3 : Comparison of the water distribution along the X axis in the central line of the cavity

Table 3 : Comparison of Sr and δT at different static residual gravities

	Static residual gravity			
	10^{-6} g$_0$	10^{-4} g$_0$	10^{-3} g$_0$	10^{-2} g$_0$
δT	0.00011 K	0.01425 K	0.1813 K	1.63 K
Sr	0.9998	0.7213	0.2669	0.1403

As the gravity increases, the temperature profile deviates further away from the linear distribution, and δT becomes very significant at high residual gravities. Meanwhile, at these conditions the Soret separation can not be fully developed due to the remixing of the mixture components, therefore Sr drops quickly below 1 and can only reach very limited values at high gravities.

As stated earlier, mass transport is a slow process in the presence of Soret effect. It is interesting to examine the relationship between the molecular diffusion characteristic time τ_D and the time required for the system to reach the mass equilibrium at different levels of gravities. Tab. 4 summarizes the results. We notice that at zero gravity and 10^{-6}g$_0$ the mass equilibrium of the system establishes on τ_D. As the static residual gravity increases the time needed for establishing the mass equilibrium reduces greatly. This may be attributed to the contribution of convection to the mass transport. At zero and microgravity conditions, the mass transport is purely due to thermal diffusion as a result of the temperature gradient. As the gravity increases, the buoyancy force becomes stronger and tends to prevent the Soret separation. The two driving forces of the mass transport – diffusion and convection – balance at a certain point and the system therefore reaches the equilibrium. At high levels of gravities, the convection far overcomes the diffusion and speeds up the fluid remixing dramatically. As a result, the system reaches the equilibrium much faster than it does at the pure or nearly pure diffusion conditions. τ_D can only be regarded as a close estimation of the time the system requires to reach the mass equilibrium at zero and microgravity conditions. This concept is of importance when estimating the necessary physical time required for numerical simulations and experiments. With τ_D as the indicator for zero gravity, simulations for zero and microgravity conditions should cover a period of time comparable to τ_D or longer. However, at higher levels of gravities, it is reasonable to reduce the physical time for simulations to some extent in order to save the scientific

negative Soret coefficient water as the reference matter (carrier) migrates to the hot wall, and isopropanol to the cold wall. At zero gravity, the concentration of water distributes linearly along the direction of the temperature gradient from the hot wall to the cold wall (graph not shown). This linear concentration profile doesn't change very much at 10^{-6}g$_0$although locally small deformations have indeed been observed. With further increase of the gravity level, the effect of buoyancy convection becomes significant. The smooth and linear concentration profile is greatly distorted at 10^{-4}g$_0$. When the gravity increases to 10^{-3}g$_0$, a boundary layer structure appears in the concentration profile: along the direction of the temperature gradient the mass separation mainly takes place in the vicinity of the hot and cold walls; while in the centre of the cubic cell it is almost homogenous. The thickness of the boundary layers is about 2 mm in this case. This phenomenon reveals the fact that the residual gravity is responsible for mixing in the cavity due to the effect of the buoyancy force. As the magnitude of the residual gravity increases further towards the ground gravity, such mixing tends to become very dramatic and the boundary layer structure becomes more distinct. The thickness of the boundary layer reduces with increase of the residual gravity, as shown in Fig. 3, which compares the water concentration along the X axis in the central line of the cavity for 10^{-3}g$_0$and 10^{-2}g$_0$.

The strong effect of the buoyancy convection can be evaluated quantitatively through the maximum temperature deviation δT and the Soret separation Sr . Tab. 3 compares δT and Sr under different static residual gravities.

Table 4 : Time required for water-isopropanol to reach the mass equilibriums at different static residual gravities

| Gravity	zero	$10^{-6}g_0$	$10^{-4}g_0$	$10^{-3}g_0$	$10^{-2}g_0$
Time to reach the mass equilibrium	32 hours	32 hours	22 hours	8 hours	50 min.

manpower.

4.2 Effect of pure oscillatory g-jitters

Three pure oscillatory g-jitter cases, as specified in Tab. 2, are investigated. The frequencies are selected in a way such to establish scales of different characteristic times. In Case 1, the oscillation period of the external vibration is $\tau_{os} = 1/f = 40s$, which is smaller than any characteristic times, τ_v (70s), τ_{th} (770s) and τ_D (115x10^{3}s) for this mixture. In Case 2, $\tau_v < \tau_{os} = 200s < \tau_{th}$; and in Case 3, $\tau_{os} = 1000s > \tau_{th}$. The rational for simulating these cases is to study the effect of different range of low-frequency vibrations on thermal diffusion.

Fig. 4 compares the time variation of water concentration for Case 1 to Case 3 at P1, which is located close to the hot wall at x =1.3mm, y = 5mm, z = 5mm (see Fig.1). Although in all cases local oscillations are observed, it is more noticeable at the frequency of 0.001Hz rather than at the other two higher frequencies. The mean values depart further away from zero-g as the g-jitter frequency decreases. By examining the concentration contours, Fig. 5(a), we notice a strong deformation of water distribution at the g-jitter with frequency of 0.001Hz. As a comparison, the water concentration contours at the higher frequency g-jitter (0.025Hz) has only been slightly distorted from the linear shape. This definitely suggests that low frequency g-jitters have a tremendous effect on Soret diffusion process. The temperature profiles, Fig. 5 (b), have also been affected by g-jitters; however, the frequency variation seems to have a less dramatic effect on the heat transfer process.

Tab. 5 and Tab. 6 quantitatively compare Sr and δT at these g-jitter conditions, respectively. At all frequencies, both Sr and δT fluctuate with time and approach asymptotically to quasi-equilibrium values as the time prolongs. This is easy to understand if we recall the fluctuation pattern of the concentration and temperature distributions. We also notice a phase shift in Sr and δT. Both Sr and δT do not respond synchronously to the excitation of the g-jitters. Furthermore, the oscillation frequencies of Sr (if any) and δT double the frequency of the external ex-
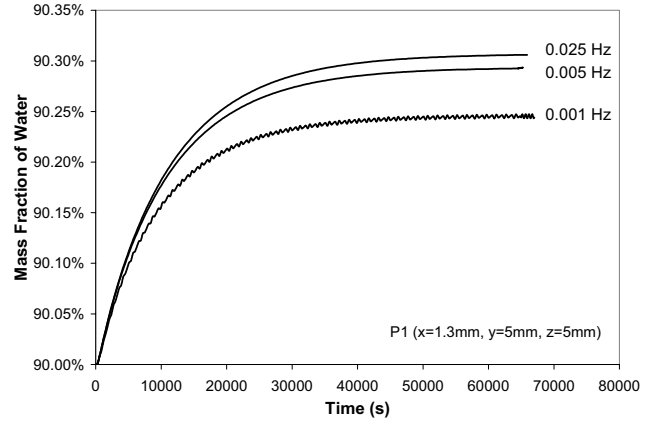
Figure 4 : Water concentration variation with time

citation. At higher frequencies of 0.025Hz and 0.005Hz, however, the oscillations of Sr are considerably weak and may be negligible. As the frequency decreases to a few thousandths of a hertz, the output oscillations become much stronger. This can be seen from the amplitudes of the local oscillations. In terms of the mean values, both Sr and δT depart further away from the ideal zero gravity values as the g-jitter frequency decreases.

4.3 Effect of combined static and oscillatory g-jitters

In reality, g-jitters are random and may consist of both static and oscillatory components simultaneously. In order to understand the fluid diffusion behaviors under these conditions, we further simulate two cases, Case 4 and Case 5 as specified in Tab. 2. In both cases, the static component of the g-jitters maintains the magnitude of 10^{-4} g_0; while the frequency changes with Case 4 ($f = 0.025$Hz) representing a higher frequency vibration and Case 5 ($f = 0.001$Hz) a lower frequency vibration.

It is anticipated that with the addition of a non-zero static residual gravity, the buoyancy convection becomes much stronger than the one induced by pure oscillatory gravities alone. Such change is, first of all, reflected in the local velocity profile, see Fig. 6. When there exists only the oscillatory g-jitter, for example in Case 1, the veloc-

Table 5 : Comparison of *Sr* at pure oscillatory g-jitter cases after 18 hours of physical time

	Case 1 (0.025Hz)	Case 2 (0.005Hz)	Case 3 (0.001Hz)
Sr (mean value)	0.9457	0.9205	0.8376
Deceased from its corresponding static case 0-g	5.4%	7.95%	16.2%
Oscillation in *Sr*	negligible	negligible	yes
Frequency of *Sr* oscillation	-	-	0.002Hz
Amplitude of *Sr* oscillation	-	-	2.38×10^{-4}

Table 6 : Comparison of δT at pure oscillatory g-jitter cases after 18 hours of physical time

	Case 1 (0.025Hz)	Case 2 (0.005Hz)	Case 3 (0.001Hz)
δT (mean value)	0.0159 K	0.0424 K	0.0706 K
Oscillation in δT	yes	yes	yes
Frequency of δT oscillation	0.05 Hz	0.01 Hz	0.002 Hz
Amplitude of δT oscillation	6.74×10^{-3} K	31.99×10^{-3} K	46.78×10^{-3} K

(a). Water concentration contours   (b) Temperature contours
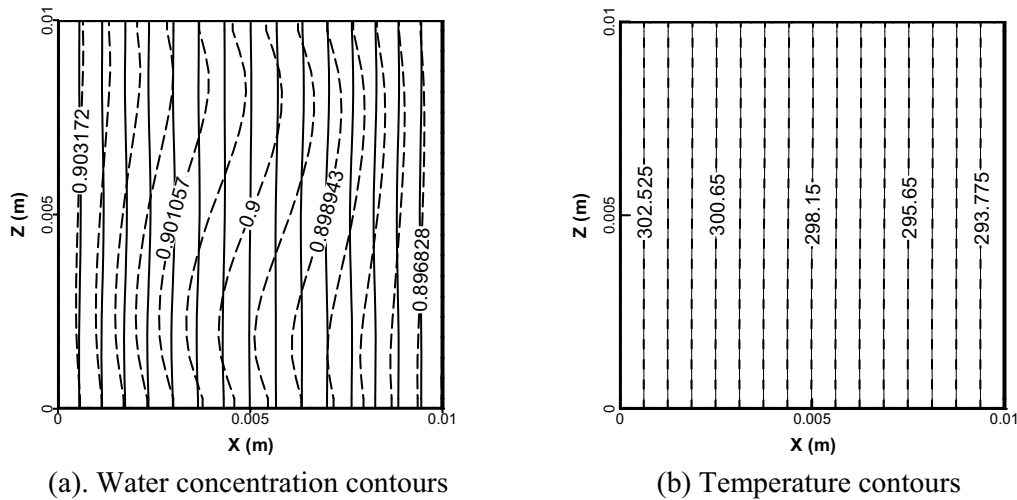
Figure 5 : Comparison of concentration and temperature contours (Case 1: solid lines; Case 3: dashed lines)

ity is symmetric with respect to the time axis and changes in a sinusoidal shape. However, in the case of combined static and oscillatory gravities, for example in Case 4, the velocity plot shifts toward the negative Z axis (the direction of the static component of the g-jitter) with a mean value not equal to zero. In addition, the amplitude of the velocity oscillation increases noticeably compared to that in the pure oscillatory g-jitter case.

Tab.7 compares the velocity fluctuation for different g-jitter cases. The data shown in this table suggest that the static gravity is not really "static" when interacting with the oscillatory g-jitter. Its existence can not only generate a stronger mean fluid flow (compared to where the static gravity is absent) in the order similar to that generated by its corresponding static gravity. It can also enhance the fluctuation of the fluid flow and cause stronger vibrations than the pure g-jitter alone. We have further noticed that in both pure oscillatory g-jitter cases and combined

Table 7 : Comparison of the velocity in Z axis, Vz, at the location P1 (after 18 hours of physical time)

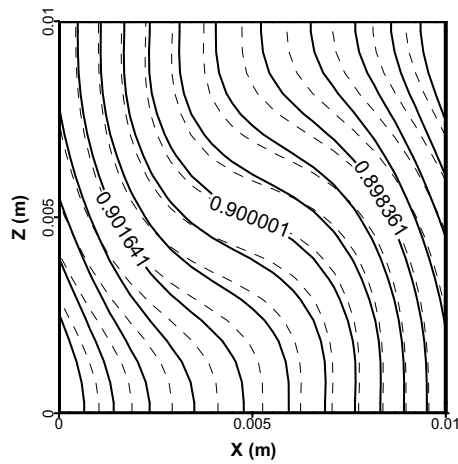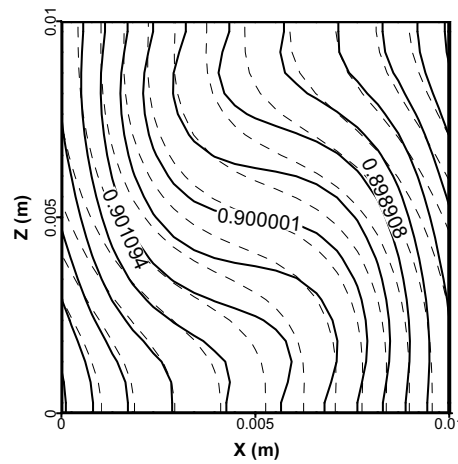|	Vz (mean value)	Frequency of Vz oscillation	Amplitude of Vz oscillation
Case 1	0	0.025Hz	4.44×10^{-6} m/s
Case 2	0	0.005Hz	4.93×10^{-6} m/s
Case 3	0	0.001Hz	5.40×10^{-6} m/s
Case 4	-0.6×10^{-6} m/s	0.025Hz	5.52×10^{-6} m/s
Case 5	-0.7×10^{-6} m/s	0.001Hz	6.18×10^{-6} m/s
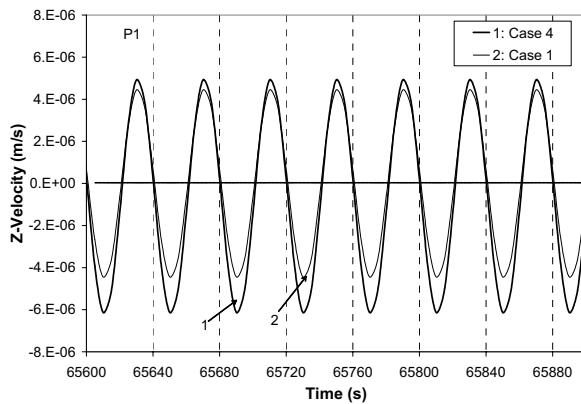
(a). Case 4 vs. Case 1
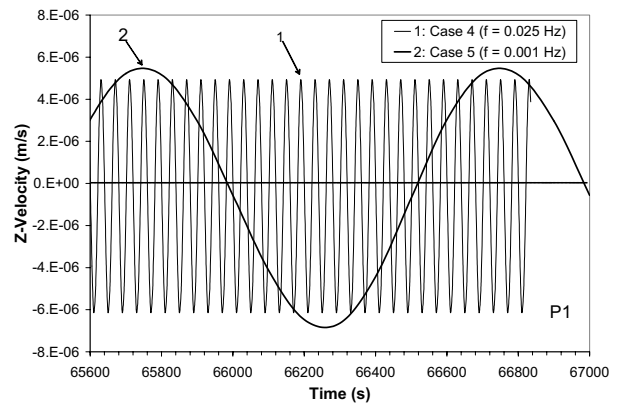
(b). Case 4 vs. Case 5

Figure 6 : Comparison of velocity variation with time at the location P1 for different cases

(a)

(b)

Figure 7 : Comparison of concentration contours: (a). Case 4 (solid lines) vs. static $g_{st} = 10^{-4} g_0$ (dashed lines) (b). Case 5 (solid lines) vs. static $g_{st} = 10^{-4} g_0$ (dashed lines)

g-jitter cases, the fluctuation of the fluid flow intensifies as the g-jitter frequency decreases. We may therefore anticipate that the effect of low frequency g-jitters is considerable either alone or in a combination with static and/or high frequency g-jitter components. In all the g-jitter cases simulated, the velocity field oscillates in a frequency equal to that of the driving g-jitters.

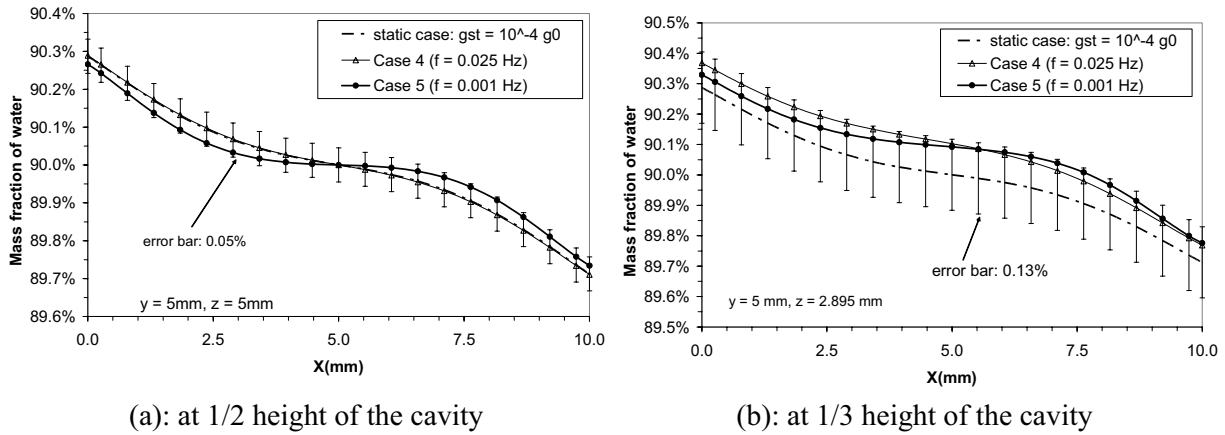Fig. 7 illustrates the water concentration contours at Case

(a): at 1/2 height of the cavity   (b): at 1/3 height of the cavity

Figure 8 : Water concentration along the X axis

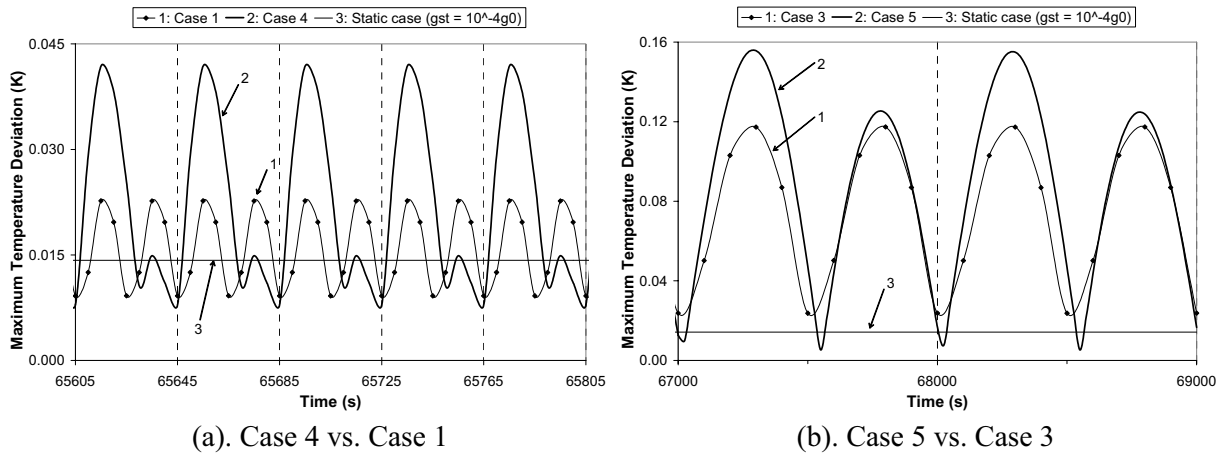(a). Case 4 vs. Case 1   (b). Case 5 vs. Case 3

Figure 9 : Comparison of δT variation with time

Table 8 : Comparison of *Sr* at cases when both static and oscillatory g-jitter exist (after 18 hours of physical time)

	Case 4 (0.025 Hz)	Case 5 (0.001 Hz)
Sr (mean value)	0.7090	0.6727
Deceased from its corresponding static case $g_{st} = 10^{-4} g_0$	1.7%	6.7%
Oscillation in *Sr* ?	yes	yes
Frequency of *Sr* oscillation	0.025 Hz	0.001 Hz
Amplitude of *Sr* oscillation	3.35×10^{-4}	93.35×10^{-4}

Table 9 : Comparison of δT at cases when both static and oscillatory g-jitter exist (after 18 hours of physical time)

	Case 4 (0.025 Hz)	Case 5 (0.001 Hz)
δT (mean value)	0.0249 K	0.0801 K
Oscillation in δT ?	yes	yes
Frequency of δT oscillation	0.025 Hz	0.001 Hz
Amplitude of δT oscillation	16.96×10^{-3} K	74.81×10^{-3} K

4 and Case 5 after the system reaches the quasi steady state. A comparison with their corresponding static case ($g_{st} = 10^{-4}g_0$) is also shown in this plot. It is obvious that with the presence of the oscillatory g-jitter component, the water distribution has been further distorted compared to that when only the static residual gravity exists; and the degree of such distortion increases as the frequency of the oscillatory g-jitter decreases. This is caused by the vibrational convection due to the oscillatory component of the g-jitter. Such vibrational convection induces an extra disturbance on the fluid flow in addition to that caused by the static residual gravity. The Soret separation is thus affected by the total effect of both static and oscillatory gravities. The fact that the concentration contour is distorted much significantly at a lower frequency g-jitter indicates a stronger vibrational convection generated by the lower frequency g-jitters than by the higher frequency ones. If we recall that the same tendency has also been observed at the pure oscillatory g-jitter cases, we may conclude that low frequency g-jitters have a much harmful effect on diffusion process regardless of the existence and/or the magnitude of static residual gravities. The effect of low frequency g-jitters is also evident from Fig. 8, where the water concentration is presented along the X axis (direction of the temperature gradient). It can be seen that the off-central locations experience a much stronger convection than the central line of the cavity. This is true for both cases, $f = 0.025$Hz and $f = 0.001$Hz, with the latter being affected more significantly. Moreover, at the lower frequency case $f = 0.001$Hz, even the central line shows a strong departure from its corresponding static residual gravity case. Since in both cases, the convection contributed by the static gravity is the same, these findings may only be explained as the result of different levels of vibrational convections related to the oscillatory part of g-jitters with different frequencies.

The temperature distortion is not obvious from the temperature contours. We plot the maximum temperature deviation δT instead to illustrate the effect of convection. Fig. 9 compares δT during the last few periods of time evolution for different cases. The value of δT at the static residual gravity case is also plotted as a reference. It is very obvious that when both the static and oscillatory gravities exist, the behavior of the temperature changes greatly in terms of both intensity and duration. The mean values of the temperature fluctuations increase sharply
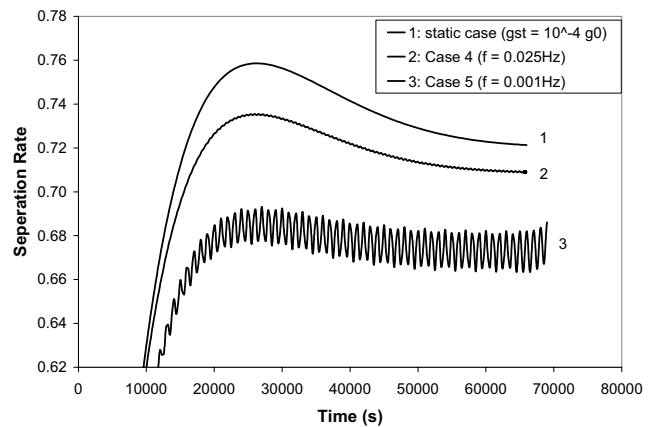

Figure 10 : Separation rate variation with time

as well as the amplitudes. In addition, a secondary oscillation appears; and such oscillations become increasingly strong as the frequency of g-jitter decreases, see the plots for Case 4 and Case 5 in Fig. 9. The change of the temperature magnitudes and patterns clearly demonstrates the strong effect of convection and the nonlinear interaction between the static and oscillatory gravities.

A quantitative evaluation of the combined effect of static and oscillatory g-jitters on diffusion may be given through the separation rate, Sr . Fig. 10 compares the time evolution of Sr for both Case 4 and Case 5 with the static case as the comparator. It is interesting to note that during the whole period of the evolution, Sr in the lower frequency case, Case 5, shows a very strong oscillation. The oscillation of Sr in Case 4, however, is considerably small. Tab. 8 compares the values of Sr for these two cases. In Case 5 the amplitude of Sr oscillation is almost 30 times larger than that in Case 4. We also notice that, by comparing Tab. 8 and Tab. 5, the amplitude of Sr oscillation is greatly enlarged in the presence of the static residual gravity regardless of the magnitude of the g-jitter frequencies. The same tendency is also found for δT if we compare Tab. 9 and Tab. 6. This again suggests that the two components of the buoyancy force, static and oscillatory, interact with each other nonlinearly; and this interaction enhances the vibrational convection, which would be induced by pure oscillatory g-jitters alone. Therefore with the existence of the static residual gravity, larger fluctuation amplitudes are shown in local parameters, such as the concentration, temperature and velocity; and these fluctuations are reflected in both Sr and δT . In terms of their mean values, both cases

have reached a much smaller separation rate, either compared with the values at the static residual gravity case or with the values at pure oscillatory cases.

In addition, we observe that when the static residual gravity exists, both concentration (i.e. *Sr*) and temperature fields oscillate in a frequency equal to that of the driving g-jitter excitation. This is very different from the pure oscillatory g-jitter cases. The reason for that is not clear yet. However, we may relate this phenomenon to the relative importance of the convection intensities induced by the static residual gravity and the oscillatory g-jitter component. If we compare the values of *Sr* in a set of cases, say, Case 1, Case 4 and the static case $g_{st}=10^{-4}g_0$, or Case 2, Case 5 and the static case $g_{st}=10^{-4}g_0$, we may notice that the values of *Sr* in Case 4 and Case 5 are very close to that in their corresponding static case ($g_{st} = 10^{-4}g_0$). This implies that at the level of $10^{-4}g_0$ the convective effect of the static component is dominant; and the oscillatory g-jitter can be regarded as a disturbance to the main flow. The dominance of the large static convection, on one hand, intensifies the overall convection, thus resulting in enlarged amplitudes in local parameters as discussed earlier. On the other hand, it tends to stabilize the main flow, therefore further perturbations are suppressed and the local oscillations are limited in a frequency identical to the external excitation.

5   Conclusions

G-jitters are unavoidable sources of convection during diffusion-dominated fluid science experiments in the Space. In this paper we have studied the effect of both static and oscillatory gravities on diffusion with a particular focus on low frequency g-jitters. A three-dimensional numerical model has been introduced within the framework of a finite volume method to solve the governing equations. Different scenarios have been studied with respect to the amplitude and frequency of the g-jitters, which may exist alone or simultaneously with static residual gravities. The effect of g-jitters on the intensity of the fluid flow, temperature distribution, solutal transport and Soret separation has been thoroughly investigated. Several conclusions may be drawn:

1. The overall effect of vibrations on diffusion is in essence a combination of the effect caused by each individual g-jitter component. However, the interaction between different g-jitter components such as the static and oscillatory components is nonlinear, which makes the phenomenon of double diffusion convection rather complicated.

2. The static residual gravity may cause a very strong fluid flow depending on the magnitude of the residual gravity. Convection thus arises and remixes the fluid mixture, resulting in an imperfect developed Soret separation. This is especially pronounced at large static residual gravities. Under such conditions, the accuracy of the diffusion measurement will be affected significantly. Large static residual gravity is definitely the most hazardous factor in diffusion measurements.

3. In the presence of oscillatory g-jitters the flow field is characterized by the oscillating convection, which has a frequency identical to the external g-jitter excitation. The flow field is enhanced when the static residual gravity exists simultaneously with the oscillatory g-jitter component in the direction perpendicular to the temperature gradient. The effect of convection on the concentration distribution becomes very dramatic especially when the g-jitter oscillates in a low frequency no matter the static residual gravity is present or not. This in turn affects the fluctuation of the Soret separation in terms of its mean value and amplitude. Similarly, the convection also affects the temperature field, which shows a larger deviation (mean value) from the ideal linear distribution as the g-jitter frequency decreases. In addition, as the frequency decreases the fluctuation in the temperature field becomes increasingly strong. In summary, low frequency g-jitters have more harmful effect on diffusion than high frequency ones. They should be very well controlled in diffusion measurements in the Space.

Reference

Chacha M.; Saghir M.Z.; Van Vaerenbergh S.; Legros J.C. (2003): Influence of thermal boundary conditions on the double-diffusive process in a binary mix-

ture, *Philosophical Magazine*, vol. 83:17-18, pp.2109-2129.

Chacha M.; Faruque D.; Saghir M.Z.; Legros J.C. (2002): Solutal thermodiffusion in binary mixture in the presence of g-jitter, *Int. J. Thermal Science.* vol.41, no.10, pp899-911.

Chacha M.; Saghir M.Z. (2005): Solutal-thermo-diffusion convection in a vibrating rectangular cavity, *Int. J. Thermal Sciences*, vol.44, pp.1-10.

Chen W.-Y.; Chen C. F. (1999): Effect of gravity modulation on the stability of convection in a vertical slot, *J. Fluid Mech.*, vol.395, pp327–344.

Farooq A.; Homsy G. M. (1994): Streaming flows due to g-jitter-induced natural convection, *J. Fluid Mech.*, vol.271, pp351-378.

Farooq A.; Homsy G. M. (1996): Linear and non-linear dynamics of a differentially heated slot under gravity modulation, *J. Fluid Mech.*, vol.313, pp1-38.

Hirata K.; Sasaki T.; Tanigawa H. (2001): Vibrational effects on convection in a square cavity at zero gravity, *J. Fluid Mech.*, vol.445, pp327-344.

Lappa M. (2005a): Review: Possible strategies for the control and stabilization of Marangoni flow in laterally heated floating zones, *FDMP: Fluid Dynamics & Materials Processing*, vol.1, no.2, pp171-188.

Lappa M. (2005b): On the nature and structure of possible three-dimensional steady flows in closed and open parallelepipedic and cubical containers under different heating conditions and driving forces", *FDMP: Fluid Dynamics & Materials Processing*, vol.1, no.1, pp1-19.

Melnikov D. E.; Shevtsova V. M. (2005): Liquid Particles tracing in three-dimensional buoyancy-driven flows, *FDMP: Fluid Dynamics & Materials Processing,* vol.1, no.2, pp189-199.

Monti R.; Savino R. (1995): A new approach to g-level tolerability for fluid and material science experiments, *Acta Astronautica* , vol.37, pp313.

Patankar, S.V. (1980): *Numerical Heat Transfer and Fluid Flow*, McGraw-Hill, New York

Peyret R.; Taylor T. D. (1983): *Computational Methods in Fluid Flows*, Springer, New York

Rees D.A.S.; Pop I. (2001): The effect of g-jitter on free convection near a stagnation point in a porous medium. *Int. J. Heat Mass Transfer*, vol.44, pp.877.

Savino R.; Lappa M. (2003): Assessment of thermovi-brational theory: application to g-jitter on the Space Station. *J. Spacecraft and Rockets*, vol. 40, no. 2, pp.201-240.

Sazonov, V. V.; Chebukov, S. Y.; Abrashkin, V. I.; Kazakova, A.E.; Zaitsev, A.S. (2004): Low-frequency microaccelerations onboard the Foton-11 satellite, *Cosmic Research*, vol. 42, no.2, pp.185-200.

Shevtsova V.; Melnikov D.; Legros J.C.; Yan Y.; Saghir M. Z.; Lyubimova T.; Sedelnikov G.; Roux B. (submitted): Influence of vibrations on thermodiffusion in binary mixture. Benchmark of numerical solutions. *Int. J. Heat and Mass Transfer*

Shu Y.; Li B.Q.; H.C. de Groh (2001): Numerical study of g-jitter induced double-diffusive convection, *Numerical Heat Transfer*, vol. 39, pp.245-265.

Shukla K.; Firoozabadi A. (1998): A new model of thermal diffusion coefficients in binary hydrocarbon mixtures. *Ind. Engrg. Chem. Res.*, vol.37**,** pp.3331-3342.